A SURVEY OF RADIATION DOSES AND INDUCED ACTIVITY AT THE ZGS
FROM SEPTEMBER 1965 TO SEPTEMBER 1966[*]

Herbert Lucks and Stewart M. Marcowitz
Argonne National Laboratory
Argonne, Illinois

Introduction

In order to know the distribution of radiation around an accelerator quantitatively, a program for monitoring the distribution of induced activity and total radiation dose in the Zero Gradient Synchrotron Ring Building was started in 1965. This paper is an attempt to compile the data to see if definite patterns exist, extract useful calculation constants, and to extrapolate the total doses received by components since the startup of the ZGS.

Some of the relationships which have been examined are:

1. the distribution of dose received by components of the ZGS per operating hour or per circulating proton;
2. the distribution of induced activity; and
3. the ratio of induced activity to average dose at the same location.

With these pieces of information, shielding designs for high intensities can be facilitated and made more economical if the radiation flux is known or can be calculated. The need for, and location of, remote handling equipment can be determined if the induced activity is known. Additional shielding requirements for personnel can be anticipated. Problems of beam loss can be localized with a knowledge of radiation distribution. Radiation damage can be anticipated and corrective action can be taken before failures occur. Component lifetimes can be estimated.

Results

The locations monitored and identification numbers are shown in Fig. 1. All dosimeters were placed near the midplane of the ZGS and the data from thermoluminescent dosimeters at these locations have been compiled and summarized. Doses and induced activities for each operating period have been compared with the number of circulating protons and operating hours for each operating period. Figure 2 shows the distribution of dose around the ZGS per operating hour at four radial positions, and the reproducibility can be seen from spreads shown at each point. These

points represent the average of the ratio of the dose accumulated during an operating period (about one month) to the number of hours in the operating period. The error bars represent the range in values. The values of dose per hour of operation (excepting the inside of the vacuum chamber) fall into roughly three groups: ~170 rads/operating hour, ~11 rads/operating hour, and ~0.8 rads/operating hour. A more detailed mapping would probably reveal some hotter locations. Similarly, the values of induced activity fall into two general groups: ~15 millirads/hour outside the vacuum chamber, and ~100 millirads/hour at hot spots.

The doses and induced activities are lower at the centers of octants because of the shielding by the ring magnet, and are lower at the walls because of distance from the source. They are peaked at every straight section at the ZGS inside. Corresponding peaking at the inside building wall is seen only at L-1, S-1, and L-3. A large fraction of the injected beam is uncaptured, and is lost uniformly about the ZGS inside as the magnetic field is increased. High energy accelerated beam is lost at L-3 (target area) and S-1 containing the first Piccioni extraction magnet. L-1 is the injection area which has an inflector. At the ZGS outside, the most prominent peaks are at S-1, L-3 and L-4 with less significant peaking at S-3, S-4 and L-1 while corresponding peaks at the wall show up only at S-1 and L-3. Reasons for peaking at S-1, L-3, and L-1 have been suggested before. The reason for the peak at L-4 is not known, but is apparently due to low energy beam loss and is probably related to the peaks at S-3 and S-4. Figure 3 shows the azimuthal variation of dose near L-3 (target area) which clearly shows the shielding effect of the ring magnet by the fall in dose at each end of the straight section.

Both the induced activity and total dose show the same general distribution pattern. Figure 4 shows the distribution of the ratio of induced activity to dose per operating hour. With a little imagination, one finds that the ratio has two general values: one about 0.75 and the other about 25. The higher value corresponds to locations with relatively large amounts of material near the dosimeter while the lower value corresponds to locations with relatively little material near the dosimeter.

Maximum average doses of about 36,000 rads per operating hour have been observed which means about 6.5×10^7 rads/year. This indicates possible radiation damage problems with the coil which is expected to fail somewhere between 10^8 and 10^{11} rads. Dosimeters in tie-rod holes, shielded by the coil itself, give readings of about 10^5 rads per operating period of about one month. Tie-rod holes go through the magnet yoke iron to the coil.

Average values per operating hour have the same distribution as average values per circulating proton; i.e., dose per circulating proton per dose per operating hour = 2×10^{-15} operating hours per circulating proton. This can be shown to be true when the circulating beam intensity is fairly constant, and this was the case during the period studied. It should be noted that the induced activity has not risen monotonically. In some cases, the lowest activities were observed late in the year.

Measurement Techniques and Calibration

Most of these data are taken from thermo-luminescent dosimeters which integrate the absorbed dose. They contain lithium flouride phosphor which has the property that radiation raises electrons in it from their ground state to metastable states, where they are trapped.[1] On heating the powder, the trapped electrons return to their ground state, emitting light, and the amount of emitted light is proportional to the radiation dose. Dose response is linear to 10^5 rads, beyond which the phosphor is permanently damaged.[2] The dosimeters are essentially dose-rate independent.

Three types of LiF phosphors are commercially available: isotopically pure flourides which contain Li^6 and Li^7 and a natural mixture of the two. These have been designated as TLD-600, TLD-700, and TLD-100, respectively. Because of the high Li^6 thermal neutron capture cross section, TLD-600 gives a much larger response in mixed beams containing thermal neutrons than TLD-700. Both are gamma and charge particle sensitive. It has been shown that the ratio of response to gamma rays to that of minimum ionizing charged particles is close to unity.[3]

A commercial thermoluminescent readout instrument was purchased (Fig. 5). Tests were made to determine the precision of the powder dispenser because the output, as read by the readout instrument, depends on the amount of powder used. It was found to dispense 28.9 mg of

LiF with a 1.7% probable error. An internal light source was used to check the reproducibility of the readout and timing cycle. Gain curves were obtained using the light source and varying the photomultiplier voltage and output gain setting. Dosimeters (Fig. 6) were exposed to a calibrated Co^{60} source. Readings from dosimeters exposed to a known dose at particular gain and voltage settings were taken and these were then combined with the gain curves to generate the dose response curves. The calibration is accurate to within 30%.

The thermal neutron response of TLD-600 was obtained by exposing TLD-600 and TLD-700. Neutrons from an americium-beryllium source, at the ANL Chemistry Division hot lab were thermalized in water. The thermal neutron flux was calibrated using standard foil activation techniques. The background was obtained from the TLD-700 capsules and subtracted from the equivalent dose registered by the TLD-600 capsules. The remaining reading was from thermal neutrons. TLD-600 was found to be 209 times as sensitive to thermal neutron dose as an equivalent dose from gammas or charged particles.

Because of the large doses at the ZGS, even the relatively small fraction (10% of the dose) of thermal neutrons give a dose equivalent beyond the linear range of the phosphor at most locations in one operating period; therefore, TLD-100 or TLD-600 is not used for obtaining the thermal neutron dose. We use TLD-700 only when neutrons are present.

An attempt was made to make the dosimeters sensitive to fast neutrons. Slurries of TLD-700 and ethanol in standard polyethylene capsules were exposed to a 14 MeV neutron beam at the ANL Chemistry Division hot lab and compared with similar dosimeters without the ethanol. It was expected that neutrons would activate the dosimeters through n-p reactions in the ethanol, but no significant difference was observed between the readings of the two sets of dosimeters. It is suspected that the dosimeters are already sensitive to fast neutrons because of the polyethylene capsule. However, we have no further knowledge of detection efficiency or sensitivity. Future investigations will be made.

Dosimeters were placed in and around the ZGS to measure the dose received during High Energy Physics experimental runs. Data were accumulated over entire operating periods of about one month each. In particular, dosimeters were placed in vacant tie-rod holes around the machine. All dosimeters were removed during the maintenance period between operating periods for reading and replaced.

At the beginning of each maintenance period, another set of dosimeters was placed around the Ring Building. These dosimeters accumulated dose from residual activity. They were removed before machine startup. Decay of induced activity around the ZGS has been observed,[4] and two approximate empirical mean lives have been calculated, which fit the decay curve. Using these, the induced activity is extrapolated from the total dose received by the capsule using the following relation:

$$\frac{I(t_o)}{D_{fi}} = \frac{K+1}{K\tau_1\left(\exp\left[-\frac{(t_i-t_o)}{\tau_1}\right] - \exp\left[-\frac{(t_f-t_o)}{\tau_1}\right]\right) + \tau_2\left(\exp\left[-\frac{(t_i-t_o)}{\tau_2}\right] - \exp\left[-\frac{(t_f-t_o)}{\tau_2}\right]\right)}$$

where,

$I(t_o)$ = the induced activity in rads/hour at time t_o,

t = time from shutdown in hours,

τ_1 = empirical mean life of 7.75 hours,

τ_2 = empirical mean life of 111 hours,

t_i = the time of dosimeter installation,

t_f = the time of dosimeter removal,

D_{fi} = the dose accumulated in rads,

and $K = (N_1 \tau_2)/(N_2 \tau_1)$

where N_1 and N_2 are the initial number of nuclei of species 1 and 2, respectively. All of our results have been taken for $t_o = 2$ hours.

Future Plans

To extend the range of measurements beyond 10^5 rads, cobalt glass dosimeters will be used.[5] The change in absorption coefficient of glass to different wavelengths of light, as measured with a spectrophotometer, is a measure of the dose received.[6,7,8] Cobalt glass can be used to 10^7 rads. We have already used glass dosimeters as a check on thermoluminescent dosimeters at doses above 10^5 rads. Bismuth silicate glass will be used to extend the range to 10^9 rads if necessary.

Cases of suspected radiation damage have been reported here. The beam bumper magnet coil in L-3 has failed; transistors and diodes in TV cameras have failed; "O" rings at several locations have hardened and caused vacuum failures. The radiation to the magnet coil may cause damage. Therefore, we will continue to monitor doses to components and expand this program where possible. Unfortunately, precise information on radiation damage to components is not generally available in the literature.[10-16] Radiation failure described in the literature does not fit an operational definition of failure: malfunction of a component due to radiation which causes an unscheduled machine shutdown or delay in an experiment. Therefore, plans are being made for systematic irradiation of materials and components to study changes in their properties with dose. The dose rates, used to irradiate samples of materials, will be sufficiently low as to avoid thermal degradation.

References

1. Karzmark, White, and Fowler, Physics in Medicine and Biology 9, 273 (1965).

2. Cameron, et al., Health Physics 10, 25 (1964).

3. Wingate, Tochilin, and Goldstein, Response of LiF to Neutrons and Charged Particles, USNRDL-TR909.

4. Dvorak, Wheeler, and Mundis, First Symposium on Accelerator Radiation Dosimetry and Experience, TLD-4500, Conference 651109, p. 33 (1965).

5. H. Lucks, S. M. Marcowitz, and D. R. Roberts, Calibration of a Glass Dosimetry System for Use Above 10^5 Rads, HL/SMM/DRR-1, Internal Report (1966).

6. Shulman, Klich, and Rabin, Nucleonics 14 (No. 1), 56 (1956).

7. Kreidl and Blair, Nucleonics 14 (No. 1), 56 (1956).

8. Hart, et al., UN Second Geneva Conference on Peaceful Uses of Atomic Energy, Vol. 21, 188 (1958).

9. Rye and Hensler, Gamma Dosimetry in a Mixed Radiation Field Above 10^6 Roentgens, Presented at the Nuclear Radiation Effects Conference at the University of Washington, July 20, 1964.

10. Harwood, et al., Effects of Radiation on Material, Reinhold (1958).

11. A. Charlesby, Atomic Radiation and Polymers, Pergamon Press (1960).

12. Bolt and Carroll, Radiation Effects on Organic Materials, Academic Press (1963).

13. Kircher and Bowman, Effects of Radiation on Materials and Components, Reinhold (1964).

14. Collins and Calkins, Radiation Damage to Elastomers, Plastics and Organic Liquids,

Apex 261, General Electric Company, Atomic Products Division (1956).

15. Kerlin and Smith, Measured Effects of Various Combinations of Nuclear Radiation Vacuum and Cryotemperatures on Engineering Materials, Annual Report Vol. I and II FXK 188-2 (NA S8-2450).

16. Broadway and Palinchak, The Effect of Nuclear Radiation on Elastomers, Plastic Components and Materials, REIC Report No. 21 (Addendum) (1964).

Fig. 1 Location and Identification of Dosimeters
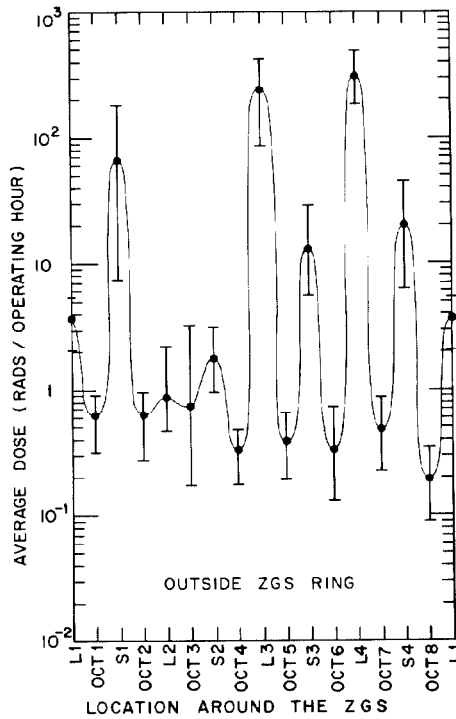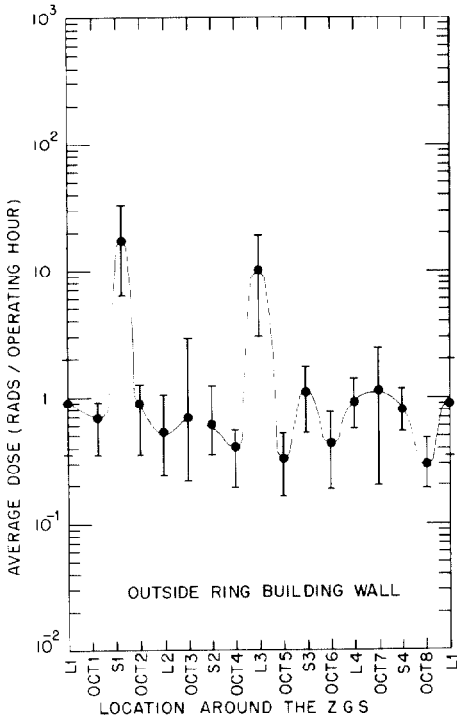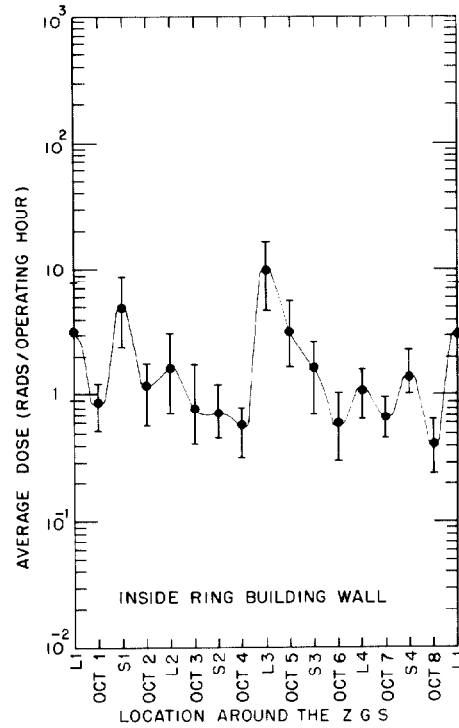

Fig. 2A
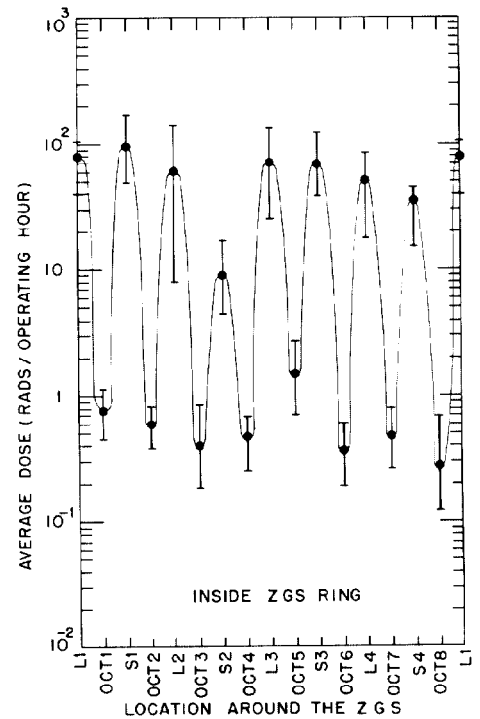
Fig. 2B

Fig. 2C

Fig. 2D

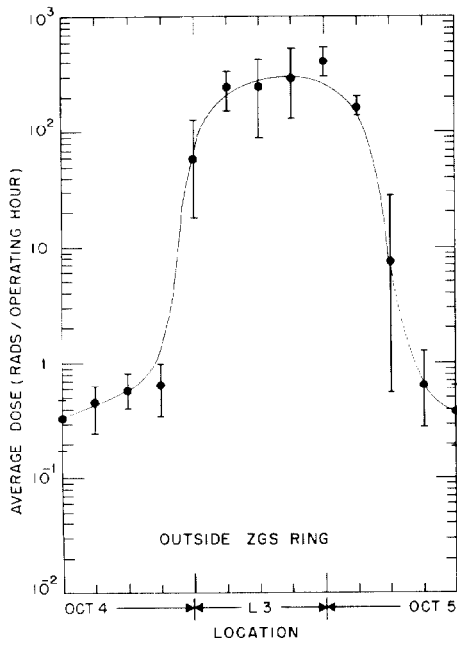Fig. 2 Radiation Doses
About the ZGS at Four
Radial Positions

Fig. 3 Average Doses
About the Target Area
at the Surface of the
ZGS Outer Radius Side

Fig. 4 The Ratio of the
Average Induced Activity
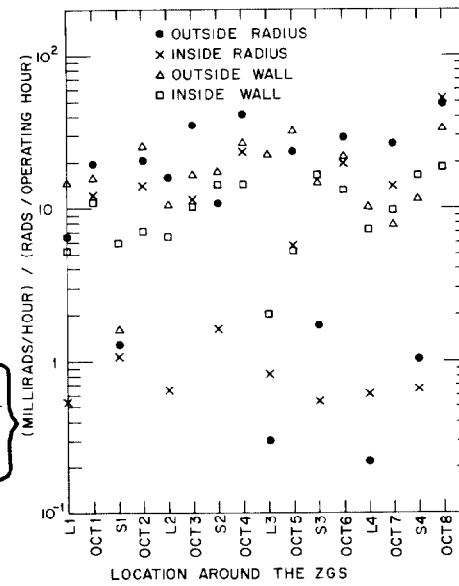to the Average Dose
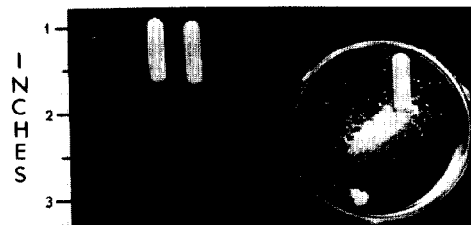per Operating Hour

Fig. 5 TLD Readout
Instrument

Fig. 6 TLD Dosimeters Com-
posed of two parts: A Poly-
ethylene Jacket, and Powder